Electronic Supplementary Material (ESI) for Journal of Materials Chemistry A.

Supporting Information

A New Strategy for Air-Stable Black Phosphorus Reinforced PVA Nanocomposites

Hong Ni†, Xiaochen Liu†, Qunfeng Cheng*

Key Laboratory of Bio-inspired Smart Interfacial Science and Technology of Ministry of Education, School of Chemistry

Beijing Advanced Innovation Center for Biomedical Engineering

Beihang University, Beijing, 100191, P. R. China

*Correspondence should be addressed to Qunfeng Cheng, E-mail: cheng@buaa.edu.cn

† These two authors contributed equally to this work

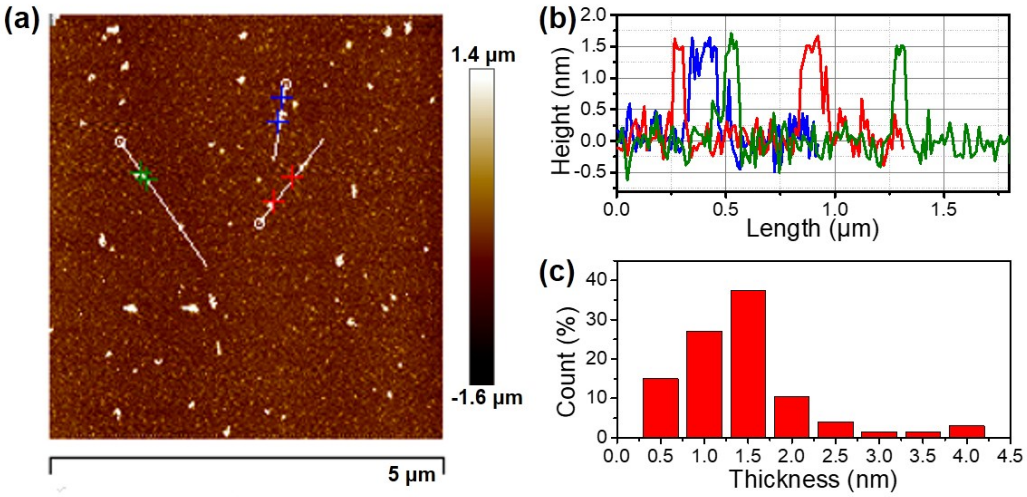

Fig S1. (a) AFM image of exfoliated BP nanosheets. (b) The specific height of the BP nanosheets signed by the corresponding color in the image (a). (c) Statistical analysis of the thickness of the exfoliated BP nanosheets measured from AFM.

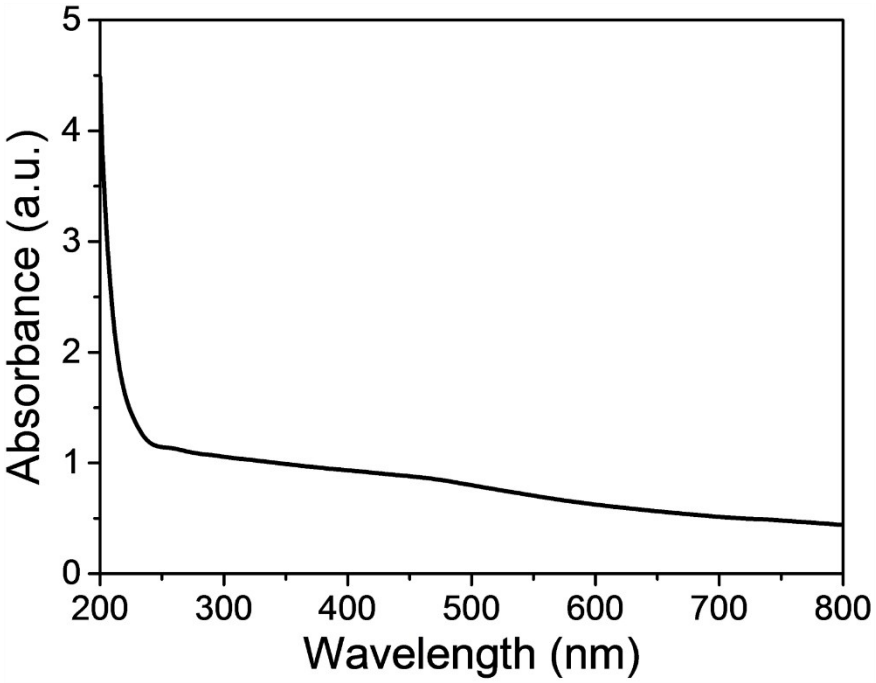

Fig S2. Absorbance spectra of BP exfoliations performed by UV–vis spectroscopy at 468 nm with the absorbance coefficient of 15 lg^{-1} cm^{-1}.

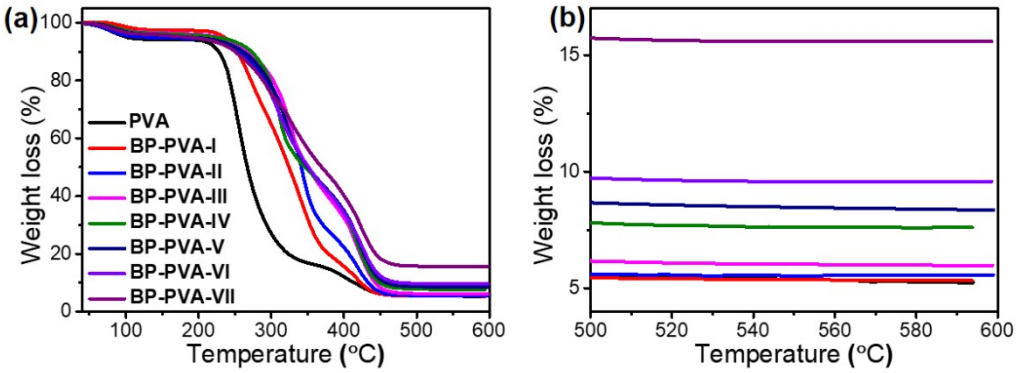

Fig S3. (a) TGA curves of PVA film, and the prepared BP-PVA-I, BP-PVA-II, BP-PVA-III, BP-PVA-IV, BP-PVA-V, BP-PVA-VI and BP-PVA-VII nanocomposites. (b) The magnification of the dash line portion in TGA curves (a), exhibiting the BP-PVA nanocomposites with different BP contents.

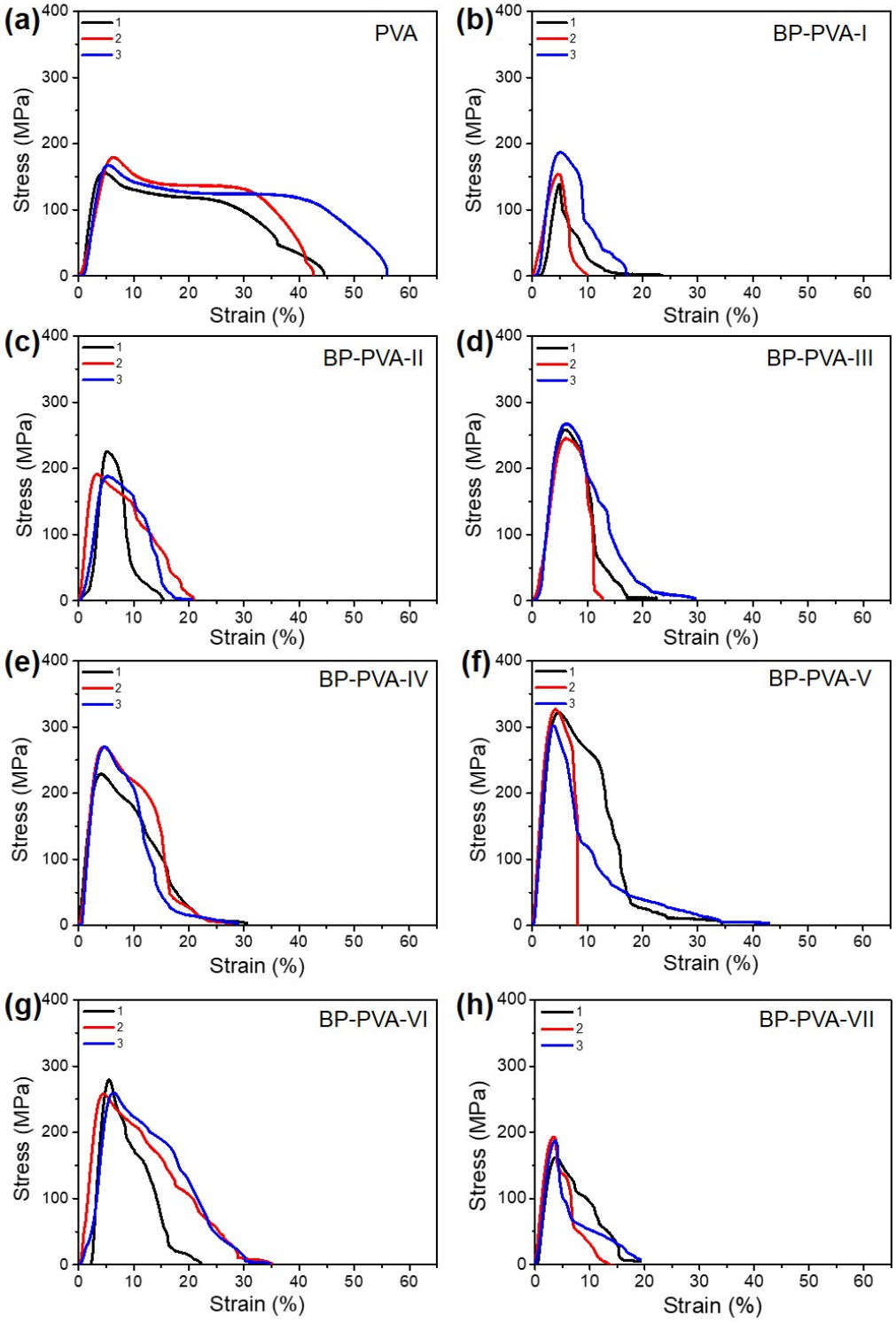

Fig S4. Stress-strain curves of (a) PVA, (b) BP-PVA-I, (c) BP-PVA-II, (d) BP-PVA-III, (e) BP-PVA-IV, (f) BP-PVA-V, (g) BP-PVA-VI and (h) BP-PVA-VII nanocomposites respectively. The curves (No.1, 2, 3) with different colors of each sample represent three parallel specimens.

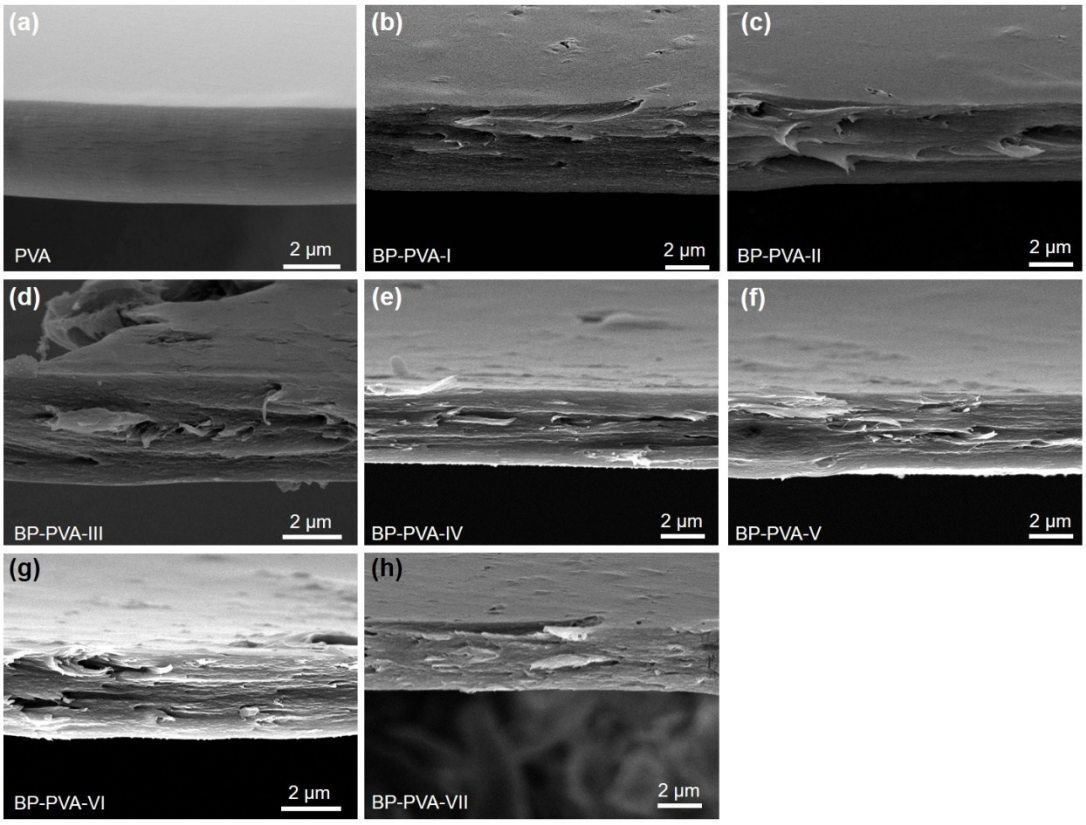

Fig S5. SEM images characterize the fracture surface of (a) PVA, (b) BP-PVA-I, (c) BP-PVA-II, (d) BP-PVA-III, (e) BP-PVA-IV, (f) V BP-PVA-V, (g) BP-PVA-VI and (h) BP-PVA-VII nanocomposites, respectively.

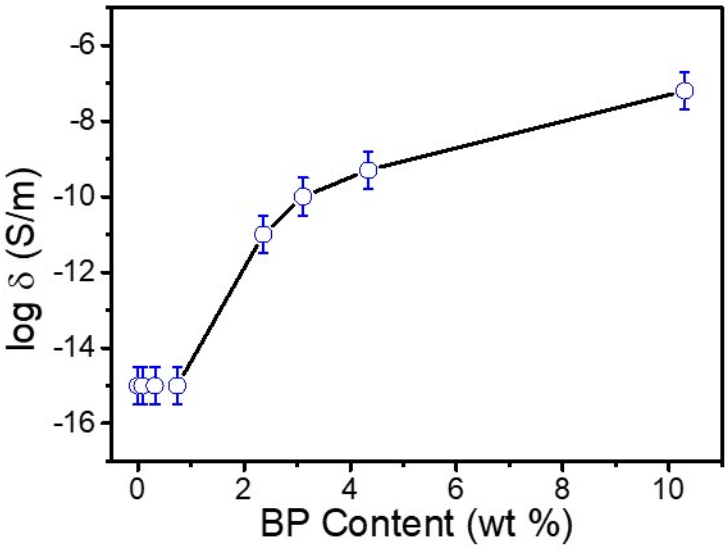

Fig S6. The electrical conductivity of PVA, BP-PVA-I, BP-PVA-II, BP-PVA-III, BP-PVA-IV, BP-PVA-V, BP-PVA-VI and BP-PVA-VII nanocomposites, respectively.

Table S1. The precise content of BP nanosheets in BP-PVA nanocomposites characterized by TGA.

Sample	BP content (wt %)
BP-PVA-I	0.08
BP-PVA-II	0.32
BP-PVA-III	0.74
BP-PVA-IV	2.36
BP-PVA-V	3.11
BP-PVA-VI	4.34
BP-PVA-VII	10.3

Table S2. Mechanical properties of PVA, BP-PVA-I, BP-PVA-II, BP-PVA-III, BP-PVA-IV, BP-PVA-V, BP-PVA-VI and BP-PVA-VII nanocomposites, respectively.

Sample	Tensile strength (MPa)	Toughness ($MJ \cdot m^{-3}$)	Young's modulus (GPa)
PVA	168.2 ± 12.1	51.7 ± 9.7	5.6 ± 1.4
BP-PVA-I	175.4 ± 25.8	9.6 ± 4.9	5.8 ± 1.2
BP-PVA-II	203.0 ± 21.1	18.2 ± 4.6	6.6 ± 0.5
BP-PVA-III	253.1 ± 12.1	22.8 ± 5.1	6.8 ± 1.6
BP-PVA-IV	258.1 ± 24.4	30.2 ± 3.0	9.4 ± 0.5
BP-PVA-V	316.9 ± 12.1	29.8 ± 10.1	11.4 ± 0.4
BP-PVA-VI	266.5 ± 13.5	35.1 ± 9.7	9.6 ± 2.3
BP-PVA-VII	179.8 ± 15.9	12.5 ± 2.1	6.3 ± 0.7

Table S3. Electrical conductivities of PVA, BP-PVA-I, BP-PVA-II, BP-PVA-III, BP-PVA-IV, BP-PVA-V, BP-PVA-VI and BP-PVA-VII nanocomposites, respectively.

Sample	Electrical Conductivity (S/m)	Log δ (S/m)
PVA	10^{-15}	-15
BP-PVA-I	10^{-15}	-15
BP-PVA-II	10^{-15}	-15
BP-PVA-III	10^{-15}	-15
BP-PVA-IV	10^{-11}	-11
BP-PVA-V	8.7×10^{-11}	-10
BP-PVA-VI	5.6×10^{-10}	-9.3
BP-PVA-VII	6.7×10^{-8}	-7.2